J. Chem. Eng. Data 1994, 39, 309–315 309

P–x and γ^∞ Data for the Different Binary Butanol–Water Systems at 50 °C

Kai Fischer and Jürgen Gmehling*

Technische Chemie, Universität Oldenburg, Fachbereich 9, Postfach 2503,
26111 Oldenburg, Federal Republic of Germany

Precise isothermal P–x data at 50 °C were measured for the different binary butanol–water systems using a static apparatus with special attention paid to the dilute region. Using these data, parameters for the different G^E models were fitted and the activity coefficients at infinite dilution were derived from the data at low concentrations using a flexible Legendre polynomial.

Introduction

The knowledge of the real behavior of butanol–water mixtures is important not only for the separation of butanol–water mixtures by rectification but also for biotechnological processes and a better understanding of the separation of butanol–water mixtures by membrane processes (e.g. pervaporation). Furthermore, precise vapor–liquid equilibrium (VLE) data for the different butanol–water systems are of interest to gain a better understanding of the influence of the molecular structure on the real behavior of mixtures. This information is important to take into account isomeric effects in group contribution methods.

A large number of VLE, liquid–liquid equilibrium (LLE), γ^∞, and heats of mixing data for butanol–water systems have been published already. A great part of these data are given in unified and evaluated form in the different volumes of the DECHEMA Chemistry Data Series (*1*). However, there is a large disagreement between γ^∞ values derived from VLE data from different researchers.

Experimental Section

Degassing and Purification. 2-Butanol, 2-methyl-1-propanol (isobutyl alcohol), 1-butanol, and 2-methyl-2-propanol (*tert*-butyl alcohol) were degassed for approximately 5 h by vacuum rectification as suggested by Van Ness and Abbott (*2*). During rectification, the reboiler temperature was kept at approximately 10 °C (30 °C in the case of *tert*-butyl alcohol) and the volatile gases were removed througha capillary at the top of the column. The completion of degassing can be judged from the metallic clicking sound in the reboiler. The disadvantage of this procedure is that without further separation less volatile impurities are enriched in the degassed liquid in the reboiler.

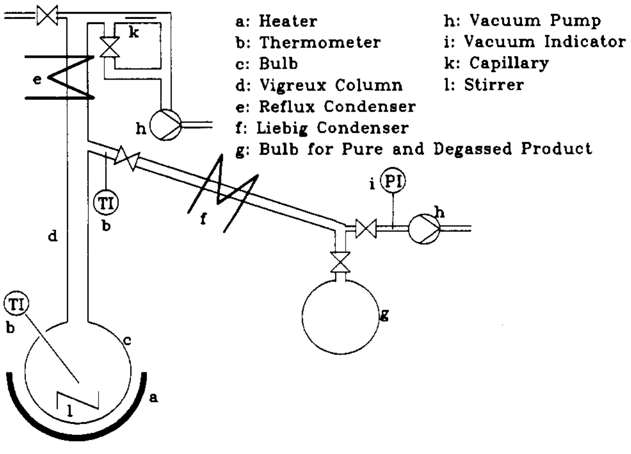

Figure 1. Purification and degassing apparatus.

Table 1. Pure Component Specifications

compound	source	water content/(wt %)
1-butanol	Riedel-de Haen	0.025,[a] <0.01[b]
2-butanol	Fluka	0.024
2-methyl-1-propanol	Henkel	0.15
2-methyl-2-propanol	Fluka	0.04

[a] First run. [b] Second run.

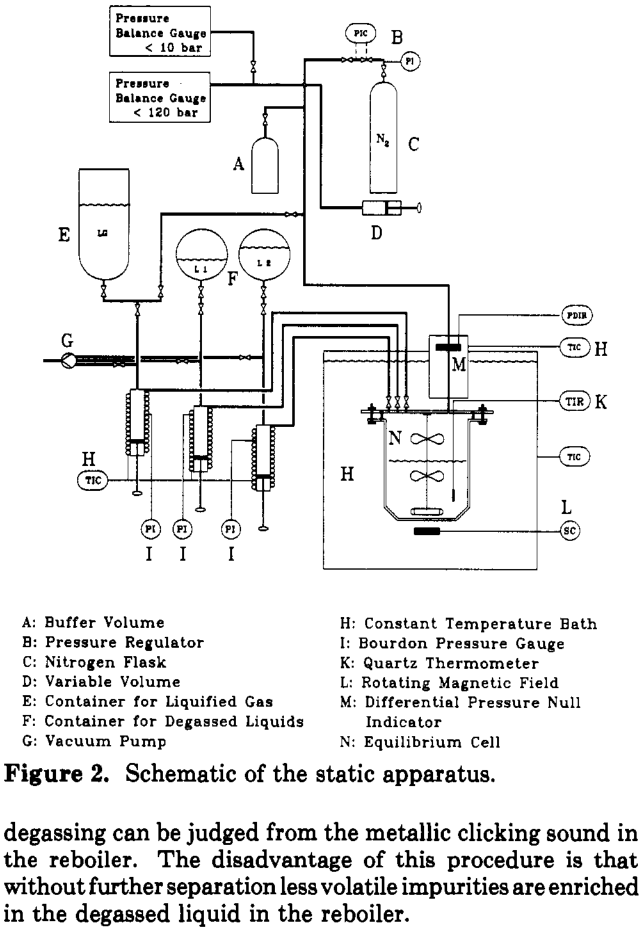

Figure 2. Schematic of the static apparatus.

Therefore, a modified degassing unit was developed (Figure 1). This unit contains a Vigreux column of 60 cm (approximately five theoretical stages). It allows chemical reactions to be carried out before degassing and the desired compound to be separated by distillation after degassing. The modified method was used to purify and degas 1-butanol by boiling with metallic sodium. The final purity of 1-butanol, deter-

0021-9568/94/1739-0309$04.50/0

Table 2. P–x Data for the System Water (1)–1-Butanol (2)

experimental		NRTL		UNIQUAC		experimental		NRTL		UNIQUAC	
x_1	P/kPa	ΔP/kPa	$y_{1,\text{calcd}}$	ΔP/kPa	$y_{1,\text{calcd}}$	x_1	P/kPa	ΔP/kPa	$y_{1,\text{calcd}}$	ΔP/kPa	$y_{1,\text{calcd}}$
First Run (T = 323.22 K)											
0.000 00[a]	4.454	0.000	0.0000	0.000	0.0000	0.401 95	14.748	0.001	0.7818	−0.311	0.7994
0.001 02	4.488	−0.023	0.0135	−0.009	0.0104	0.433 65	14.964	−0.046	0.7899	−0.095	0.8085
0.005 17	4.665	−0.073	0.0647	−0.001	0.0504	0.468 94	15.107	−0.041	0.7976	0.047	0.8165
0.010 19	4.953	−0.053	0.1193	0.081	0.0949	0.985 47	14.871	−0.277	0.7894	−0.188	0.7946
0.017 41	5.296	−0.086	0.1865	0.133	0.1520	0.988 75	14.647	−0.142	0.8148	−0.011	0.8218
0.022 31	5.561	−0.069	0.2260	0.203	0.1869	0.990 11	14.708	0.135	0.8277	0.271	0.8353
0.026 28	5.773	−0.053	0.2550	0.258	0.2132	0.991 49	14.453	0.125	0.8426	0.261	0.8506
0.038 02	6.278	−0.108	0.3279	0.306	0.2820	0.993 54	13.986	0.066	0.8688	0.195	0.8768
0.052 40	6.947	−0.084	0.3978	0.428	0.3517	0.994 91	13.963	0.352	0.8895	0.469	0.8971
0.074 38	7.941	0.002	0.4773	0.615	0.4357	0.996 29	13.442	0.174	0.9136	0.271	0.9203
0.132 22	9.958	0.021	0.6032	0.680	0.5797	0.997 69	12.810	−0.073	0.9420	−0.005	0.9470
0.217 47	12.228	0.132	0.6961	0.527	0.6939	0.998 94	12.460	−0.048	0.9714	−0.013	0.9741
0.300 50	13.650	0.090	0.7454	0.111	0.7557	0.999 33	12.439	0.055	0.9815	0.078	0.9833
0.345 26	14.225	0.072	0.7638	−0.091	0.7782	0.999 70	12.247	−0.016	0.9915	−0.006	0.9924
0.375 89	14.529	0.035	0.7741	−0.237	0.7905	1.000 00	12.163	0.000	1.0000	0.000	1.0000
0.386 76	14.585	−0.017	0.7774	−0.325	0.7944						
Second Run (T = 323.23 K)											
0.000 00	4.450	0.000	0.0000	0.000	0.0000	0.985 05	15.227	0.105	0.7915	0.243	0.8044
0.004 18	4.829	0.123	0.0581	0.208	0.0407	0.987 33	15.076	0.091	0.8062	0.380	0.8214
0.009 55	5.096	0.073	0.1222	0.260	0.0884	0.989 26	14.779	0.056	0.8215	0.357	0.8382
0.016 50	5.400	−0.016	0.1917	0.288	0.1436	0.990 97	14.483	0.030	0.8378	0.331	0.8553
0.040 26	6.509	−0.132	0.3554	0.479	0.2912	0.991 75	14.332	0.016	0.8463	0.312	0.8639
0.062 53	7.474	−0.164	0.4506	0.620	0.3903	0.992 54	14.168	−0.000	0.8556	0.288	0.8732
0.062 53	7.397	−0.242	0.4506	0.542	0.3903	0.993 31	14.003	−0.013	0.8654	0.266	0.8828
0.083 81	8.434	−0.041	0.5139	0.824	0.4624	0.994 09	13.816	−0.034	0.8762	0.230	0.8932
0.104 49	9.183	−0.013	0.5597	0.872	0.5180	0.994 87	13.648	−0.027	0.8880	0.220	0.9043
0.123 93	9.817	0.014	0.5933	0.874	0.5607	0.995 49	13.500	−0.027	0.8982	0.202	0.9136
0.142 56	10.360	0.033	0.6196	0.838	0.5951	0.996 11	13.344	−0.028	0.9091	0.181	0.9235
0.191 79	11.606	0.112	0.6706	0.674	0.6643	0.996 71	13.194	−0.021	0.9204	0.165	0.9336
0.233 73	12.383	0.094	0.7010	0.391	0.7064	0.997 28	13.050	−0.008	0.9320	0.153	0.9437
0.273 54	13.075	0.160	0.7232	0.195	0.7370	0.997 97	12.856	−0.001	0.9471	0.127	0.9566
0.313 81	13.599	0.152	0.7412	−0.060	0.7612	0.998 57	12.696	0.022	0.9613	0.117	0.9686
0.345 20	13.948	0.145	0.7530	−0.239	0.7765	0.998 83	12.618	0.025	0.9678	0.105	0.9740
0.379 88	14.275	0.129	0.7643	−0.414	0.7905	0.999 10	12.540	0.034	0.9748	0.097	0.9797
0.414 13	14.512	0.074	0.7741	−0.540	0.8018	0.999 29	12.480	0.037	0.9799	0.087	0.9839
0.451 72	14.691	−0.021	0.7834	−0.361	0.8117	0.999 51	12.360	−0.008	0.9859	0.026	0.9887
0.485 44	14.812	−0.107	0.7908	−0.240	0.8187	0.999 68	12.319	0.007	0.9907	0.031	0.9926
0.514 37	14.880	−0.190	0.7964	−0.172	0.8234	0.999 82	12.279	0.014	0.9947	0.028	0.9958
0.543 40[c]	14.987	−0.134	0.8015	−0.065	0.8268	1.000 00	12.200	0.000	1.0000	0.000	1.0000
0.571 40[c]	15.008	−0.113	0.8057	−0.044	0.8291			0.072[b]		0.397[b]	

[a] Calculated with the Antoine equation using the parameters listed in Table 6. [b] Mean deviation. [c] Two liquid phases.

mined by gas chromatography and Karl-Fischer titration, was better than 99.99%.

Table 1 shows the sources and water content of the pure compounds used in the measurements. The water content was determined by Karl-Fischer titration and was taken into account in evaluation of the experimental data.

Static Apparatus and Measurement Procedure. A detailed description of the static apparatus has been given previously (*3*). The equilibrium cell is thermostated using a constant-temperature bath. The feed composition can be determined by reading liquid volume changes in the piston injectors. The system equilibrium pressure is compensated using a differential pressure null indicator, which is superheated to prevent condensation. A nitrogen system is used to transduce the pressure to balance gauges.

A few improvements have been introduced.

(1) The liquids in the piston injectors are now kept at constant temperature (±0.1 K) and pressure (±0.01 bar). The constant temperature is maintained using a thermostated jacket, and the pressure is controlled by a Bourdon pressure gauge. Both changes reduce the error (temperature and pressure dependence of the density) in the feed composition of the mixture to ±0.0001 mole fraction over the whole concentration range. The thermostated pumps allow the measurements to be extended to the substances with a normal melting point above ambient temperature. Furthermore, measurements in the extremely dilute region can be performed since the injection of small amounts (down to 0.01 cm^3) is within the required accuracy. A more precise pressure measurement allows compressibilities of the liquids to be roughly determined (±5%) by recording the volume changes during compression.

(2) The upper pressure limit was extended from 10 to 120 bar by replacing the glass equilibrium cell by a steel cell and using additionally a new balance gauge (digital dynamometer type 21000 combined with pressure block type 410 from Desgranges & Huot, France).

(3) A piston-plug unit as a variable volume in the reference system simplifies the adjustment of the nitrogen pressure in the reference system to the pressure in the system using a differential pressure null indicator. Calibrations demonstrate that the measurement of the pressure can be performed now with an accuracy of (±1 mbar + 0.02% of the absolute pressure).

(4) The electric motor magnetically connected with the stirrer in the equilibrium cell has been replaced by a rotating magnetic field, induced by four solenoids.

A schematic of the apparatus is shown in Figure 2. The degassed, pure compounds are filled into the evacuated piston injectors. Then one of the pure components is filled into the evacuated thermostated equilibrium cell, and pressure and temperature are measured after equilibrium is reached.

Table 3. P–x Data for the System Water (1)–2-Butanol (2) at 323.18 K

experimental		NRTL		UNIQUAC	
x_1	P/kPa	ΔP/kPa	$y_{1,\mathrm{calcd}}$	ΔP/kPa	$y_{1,\mathrm{calcd}}$
0.000 00[a]	10.475	0.000	0.000 00	0.000	0.000 00
0.000 98	10.531	0.010	0.005 30	0.020	0.004 40
0.006 74	10.904	0.118	0.035 30	0.185	0.029 30
0.012 02	10.944	−0.076	0.060 80	0.037	0.051 10
0.018 04	11.268	−0.013	0.087 90	0.150	0.074 70
0.025 57	11.566	−0.029	0.119 00	0.187	0.102 60
0.033 37	11.855	−0.052	0.148 50	0.212	0.129 70
0.044 09	12.262	−0.053	0.105 00	0.265	0.164 30
0.055 68	12.658	−0.073	0.220 10	0.290	0.198 70
0.076 99	13.363	−0.070	0.275 10	0.343	0.254 70
0.163 15	15.655	0.054	0.420 20	0.388	0.415 60
0.296 54	17.816	0.268	0.534 60	0.198	0.551 60
0.408 65	18.574	0.184	0.588 70	−0.112	0.612 60
0.522 71[b]	18.577	−0.207	0.623 70	−0.348	0.644 70
0.622 60[b]	18.730	−0.113	0.641 40	−0.194	0.652 70
0.719 63[b]	18.777	−0.066	0.645 80	−0.148	0.642 20
0.990 38	15.296	0.059	0.793 80	0.269	0.804 70
0.992 04	14.829	0.016	0.817 60	0.215	0.828 60
0.993 71	14.341	−0.007	0.845 20	0.171	0.855 80
0.995 35	13.835	−0.017	0.876 80	0.131	0.886 30
0.997 02	13.279	−0.024	0.914 40	0.083	0.921 80
0.998 70	12.686	−0.015	0.959 20	0.037	0.963 20
0.999 56	12.323	−0.049	0.985 50	−0.030	0.987 00
0.999 82	12.263	−0.007	0.994 00	0.000	0.994 60
1.000 00	12.199	0.000	1.000 00	0.000	1.000 00
		0.072[c]		0.209[c]	

[a] Calculated with the Antoine equation using the parameters listed in Table 6. [b] Two liquid phases. [c] Mean deviation.

Table 4. P–x Data for the System Water (1)–Isobutyl Alcohol (2) at 323.15 K

experimental		NRTL		UNIQUAC	
x_1	P/kPa	ΔP/kPa	$y_{1,\mathrm{calcd}}$	ΔP/kPa	$y_{1,\mathrm{calcd}}$
0.000 00[a]	7.001	0.000	0.0000	0.000	0.0000
0.006 11	7.346	−0.008	0.0538	0.053	0.0457
0.014 08	7.754	−0.043	0.1146	0.089	0.0993
0.023 37	8.233	−0.057	0.1746	0.143	0.1544
0.032 49	8.691	−0.058	0.2247	0.195	0.2021
0.041 92	9.111	−0.088	0.2692	0.206	0.2459
0.051 62	9.550	−0.090	0.3089	0.233	0.2861
0.066 04	10.186	−0.068	0.3587	0.279	0.3381
0.083 05	10.828	−0.091	0.4068	0.256	0.3900
0.101 50	11.540	−0.036	0.4493	0.283	0.4373
0.128 23	12.568	0.144	0.4982	0.386	0.4932
0.153 80	13.167	0.036	0.5350	0.174	0.5362
0.177 57	13.831	0.120	0.5629	0.145	0.5693
0.296 78	15.955	0.183	0.6512	−0.359	0.6742
0.457 63	17.116	0.071	0.7081	0.020	0.7333
0.651 86[b]	17.127	0.082	0.7315	0.031	0.7358
0.982 11	17.231	0.186	0.6997	0.158	0.7027
0.990 80	15.469	0.035	0.7824	0.251	0.7933
0.992 52	14.960	0.000	0.8083	0.213	0.8198
0.994 24	14.409	−0.021	0.8391	0.174	0.8505
0.995 93	13.796	−0.055	0.8754	0.108	0.8858
0.997 65	13.176	−0.017	0.9205	0.093	0.9282
0.998 52	12.796	−0.037	0.9471	0.038	0.9527
0.999 07	12.587	−0.008	0.9656	0.041	0.9694
0.999 48	12.392	−0.019	0.9802	0.009	0.9825
0.999 77	12.282	0.003	0.9911	0.016	0.9921
1.000 00	12.172	0.000	1.0000	0.000	1.0000
		0.067[c]		0.231[c]	

[a] Calculated with the Antoine equation using the parameters listed in Table 6. [b] Two liquid phases. [c] Mean deviation.

Table 5. P–x Data for the System Water (1)–*tert*-Butyl Alcohol (2) at 323.13 K

experimental		NRTL		UNIQUAC	
x_1	P/kPa	ΔP/kPa	$y_{1,\mathrm{calcd}}$	ΔP/kPa	$y_{1,\mathrm{calcd}}$
0.000 00[a]	23.046	0.000	0.0000	0.000	0.0000
0.001 63	23.173	0.091	0.0031	0.103	0.0026
0.009 78	23.503	0.252	0.0184	0.317	0.0157
0.020 43	23.622	0.159	0.0375	0.289	0.0323
0.029 83	23.761	0.121	0.0534	0.302	0.0465
0.038 04	23.830	0.043	0.0668	0.265	0.0586
0.047 62	23.945	−0.005	0.0818	0.258	0.0724
0.067 65	24.214	−0.050	0.1110	0.288	0.1001
0.098 63	24.621	−0.065	0.1514	0.356	0.1399
0.204 01	25.550	−0.079	0.2575	0.428	0.2530
0.379 65	26.141	0.090	0.3708	0.503	0.3821
0.551 97	25.803	0.139	0.4383	0.448	0.4537
0.699 85	25.326	0.155	0.4681	0.163	0.4753
0.801 75	25.062	−0.067	0.4710	−0.100	0.4686
0.862 06	24.894	−0.235	0.4675	−0.268	0.4605
0.894 08	24.822	−0.307	0.4677	−0.340	0.4598
0.915 42	24.701	−0.328	0.4720	−0.461	0.4648
0.932 85	24.531	−0.070	0.4816	−0.315	0.4759
0.940 77	24.415	0.148	0.4892	−0.041	0.4845
0.948 72	24.111	0.312	0.5000	0.188	0.4966
0.956 05	23.635	0.425	0.5140	0.370	0.5122
0.962 14	23.031	0.459	0.5299	0.466	0.5296
0.967 71	22.231	0.393	0.5492	0.456	0.5504
0.971 67	21.481	0.271	0.5667	0.372	0.5691
0.975 53	20.670	0.174	0.5878	0.308	0.5914
0.979 24	19.620	−0.080	0.6130	0.078	0.6177
0.979 95	19.433	−0.101	0.6185	0.061	0.6235
0.981 54	18.940	−0.205	0.6317	−0.035	0.6372
0.985 15	17.871	−0.296	0.6675	−0.117	0.6740
0.988 15	16.865	−0.375	0.7050	−0.199	0.7121
0.991 29	15.795	−0.351	0.7547	−0.193	0.7621
0.993 00	15.156	−0.334	0.7878	−0.192	0.7951
0.994 01	14.769	−0.311	0.8099	−0.183	0.8169
0.994 98	14.399	−0.273	0.8332	−0.159	0.8397
0.995 98	14.003	−0.231	0.8596	−0.134	0.8655
0.996 97	13.592	−0.190	0.8886	−0.113	0.8936
0.997 88	13.220	−0.131	0.9181	−0.073	0.9221
0.998 86	12.764	−0.104	0.9534	−0.072	0.9558
0.999 77	12.395	−0.009	0.9901	−0.002	0.9906
1.000 00	12.284	0.000	1.0000	0.000	1.0000
		0.200[b]		0.269[b]	

[a] Calculated with the Antoine equation using the parameters listed in Table 6. [b] Mean deviation.

Before and after every injection the liquid volume left in the piston injectors is determined at the chosen conditions (P = 50 bar, T = 25 or 30 °C). To check for complete degassing, the vapor pressure is measured again after a second injection of the pure compound. After the pure component vapor pressure has been determined, the second component is injected. The equilibrium is established after approximately 30 min, and the pressure is measured for the given feed composition. This procedure is continued until approximately 60 vol % of the second compound is attained.

Then the equilibrium cell is emptied and evacuated, and the same procedure is followed with the pure component 2. After the second series, the whole concentration range is covered and the two independent parts of the isotherm should overlap.

Results

The concentration of the liquid phase is obtained from the feed composition by an iterative flash calculation. The volume of the liquid mixture is calculated from the pure component volumes at the pressure and temperature of the measurement, neglecting the excess volume. The difference of the known volume of the equilibrium cell and the volume of the liquid mixture is used to calculate the amount of moles in the vapor phase assuming ideal behavior of the vapor phase. At low pressures this assumption causes only negligible errors. The raw data (isothermal P–x data) are then fitted using a Legendre polynomial, and finally the composition of the liquid phase is recalculated using the calculated composition of the vapor phase.

Table 6. Pure Component Properties[a]

compound	r	q	ρ/(g cm^{-3})	A	B	C
water	0.9200	1.400	0.9993 (25 °C, 50 bar) 0.9980 (30 °C, 50 bar)	7.1962[b]	1730.630	233.426
1-butanol	3.4543	3.052	0.8093 (25 °C, 50 bar)	6.958	1558.190	196.881
isobutyl alcohol	3.4535	3.048	0.8057 (25 °C, 50 bar)	7.639	1950.940	237.147
2-butanol	3.4535	3.048	0.8084 (25 °C, 50 bar)	6.600	1314.188	186.500
tert-butyl alcohol	3.4528	3.128	0.7776 (30 °C, 50 bar)	6.487	1180.930	180.476

[a] r = relative van der Waals volume, q = relative van der Waals surface, ρ = density, and A, B, C = constants for Antoine equation $\log P^{s} = A - [B/(T + C)]$; P in kPa, T in °C. [b] Adjusted to the different experimental vapor pressures.

Table 7. Fitting Results

Parameters

system	T/°C	NRTL			UNIQUAC	
		A_{12}/(cal/mol)	A_{21}/(cal/mol)	α_{12}	A_{12}/(cal/mol)	A_{21}/(cal/mol)
water–1-butanol[a]	50.07	2451.52	465.53	0.3870	506.31	128.55
water–1-butanol[b]	50.08	2421.22	610.90	0.4317	487.18	129.58
water–isobutyl alcohol	50.00	2334.33	525.00	0.3931	357.64	286.89
water–2-butanol	50.03	2011.78	477.42	0.4335	245.19	284.12
water–*tert*-butyl alcohol	49.98	1764.14	326.25	0.4580	215.86	232.75

Activity Coefficients at Infinite Dilution

		activity coefficients at infinite dilution							
		quasi experimental		calculated					
		Legendre	polynomial	NRTL		UNIQUAC		reference data	
system	T, °C	1	2	1	2	1	2	1	2
water–1-butanol	50.07[a]			4.93	78.59	3.76	70.38	3.27 (70 °C) (*7*)	49.5 (40 °C) (*8*)
water–1-butanol	50.08[b]	5.2	78.7	5.43	81.47	3.70	64.52		59.3 (60 °C) (*8*)
water–isobutyl alcohol	50.0	5.3	58.1	5.41	68.57	4.51	60.29		48.4 (25 °C) (*12*)
water–2-butanol	50.03	4.6	35.5	4.71	39.30	3.85	35.05	3.54 (59 °C) (*10*)	46.49 (60.4 °C) (*1*)
water–*tert*-butyl alcohol	49.98	4.9	19.2	3.63	23.33	3.05	22.02		12.2 (25 °C) (*12*)

Azeotropic Data

system	T/°C	NRTL		UNIQUAC		reference data	
		P/kPa	x_1	P/kPa	x_1	P/kPa	x_1
water–1-butanol	50.07[a]	15.15	0.79	15.06	0.80	15.10	0.808 (50 °C) (*7*)
water–1-butanol	50.08[b]	15.12	0.80	15.05	0.80		
water–isobutyl alcohol	50.00	17.04	0.70	17.10	0.70	26.66	0.688 (60.1 °C) (*11*)
water–2-butanol	50.03	18.64	0.63	18.93	0.63	26.66	0.632 (56.95 °C) (*9*)
water–*tert*-butyl alcohol	49.98	26.06	0.36	25.64	0.38	26.41	0.350 (50 °C) (*6*)

[a] First run. [b] Second run.

This iterative procedure converges after a few cycles. For our measurements, the corrections to obtain the liquid mole fraction from the total composition are smaller than 0.0003, which is of the magnitude of the accuracy of the total composition. The experimental P–x data are listed in Tables 2–5. Since we cannot observe the mixture in the equilibrium cell optically, liquid–liquid immiscibility in binary mixtures can only be obtained from the pressure constancy in the P–x diagram. The experimental points in Tables 2–5 in the miscibility gap are marked.

The parameters for the G^{E} models NRTL and UNIQUAC were fitted with the help of the Simplex–Nelder–Mead method (*4*) using the objective function $F = \sum(P_{\mathrm{exptl}} - P_{\mathrm{calcd}})^2$ and were used to calculate the pressure and vapor composition. The obtained parameters are listed in Table 7. In Tables 2–5, the deviations $P_{\mathrm{exptl}} - P_{\mathrm{calcd}}$ and the calculated vapor compositions for these models are listed. Furthermore, in Table 7 the calculated γ_i^{∞} values and azeotropic points are compared with published experimental values. The required pure component properties used for the calculations are listed in Table 6.

Figure 3 shows the experimental P–x data and the calculated P–x–y curves calculated using the fitted NRTL parameters. In the cases of water–1-butanol and water–*tert*-butyl alcohol, the literature VLE data (*5*, *6*) at about the same temperature are plotted together with our data for comparison.

At 50 °C all butanol–water systems show a pressure maximum azeotrope. While for 1-butanol and isobutyl alcohol heterogeneous azeotropes are found, the *tert*-butyl alcohol–water and 2-butanol–water systems show a homogeneous azeotropic point.

Although in contrast to the other butanols *tert*-butyl alcohol is completely miscible with water at 50 °C, both the NRTL and the UNIQUAC models used to fit experimental data give a miscibility gap.

The systematic deviations (Tables 2–5) between experimental and calculated data for all systems show that modern G^{E} models, such as NRTL and UNIQUAC, cannot describe the big changes in the slope $\mathrm{d}P/\mathrm{d}x$, which occur at high dilution and near the miscibility gap, with the required accuracy.

Therefore, a flexible Legendre polynomial with a variable number of parameters was applied to describe the experimental data within the experimental accuracy. To obtain reliable γ^{∞} data, only a few data points (about 5–10) at high dilution were used to fit the parameters. The observed average deviation of about 0.040 kPa was close to the experimental accuracy. Then, using the slope of the P–x curve at $x = 0$ or $x = 1$, the activity coefficients at infinite dilution were calculated. The values are listed in Table 7b.

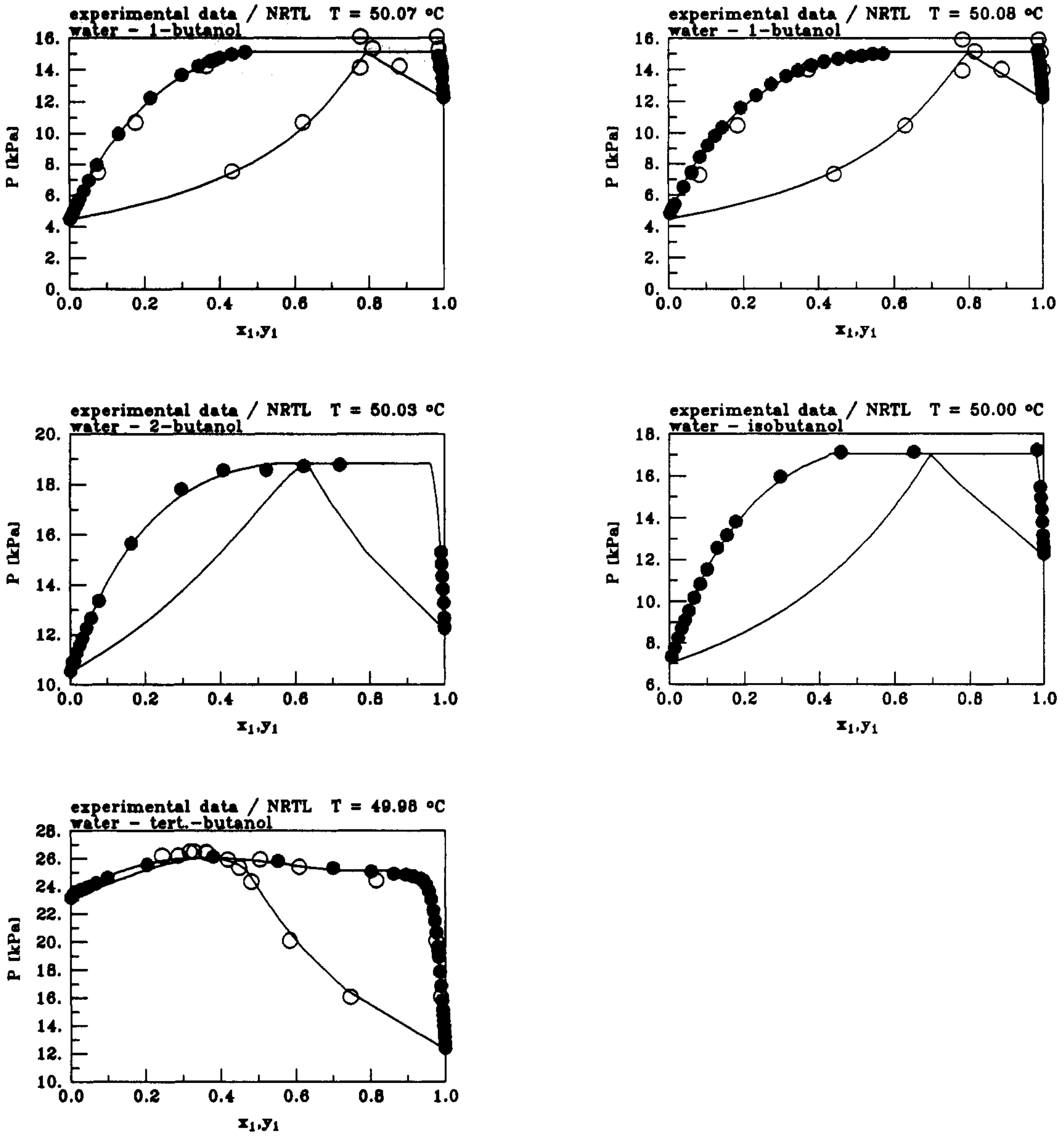

Figure 3. Experimental *P–x* data and calculated *P–x–y* behavior using the NRTL equation: (○) literature data (*5*, *6*), (●) this work.

The experimental *P–x* data and the *P–x* curves calculated using the Legendre polynomial are shown in Figure 4. Since the first VLE measurement in the system water–1-butanol (Table 2a) showed large scattering at high dilution, an electrical contact at the bourdon pressure gauge for the piston injectors was added to measure the pressure in the pumps with an increased accuracy of about 1 kPa. The results of the repeated measurements are given in Table 2b.

The γ_i^∞ values for different butanols diluted in water are listed in Table 7b. They decrease with branching of the molecules from the straight chain to the isomers, which contain tertiary or quarternary carbon atoms. This effect is stronger for hydroxyl groups than for methyl groups bound to these carbon atoms.

A decrease of γ_i^∞ values for the branched butanols is connected with an increase of their solubility in water. This means the closer the aliphatic groups are to the hydroxyl group, the better is the solubility of the alcohol in water, although the dipole moments of the different butanols have almost equal values.

On the other side, the same effect is found for the γ_i^∞ values for water in the different butanols, whereby it is independent of the branching of the carbon chains but mainly caused by the hydroxyl group.

Compared to the cited γ_i^∞ values (Table 7), all the γ_i^∞ values obtained using a flexible Legendre polynomial are greater. The reason is that for mixtures of high dilution the γ_i value shows the largest dependence on the liquid composition. As shown in Figure 4, the slope d*P*/d*x* changes by a factor of 2 during variation of the concentration only by 1 mol % at high dilution.

Conclusions

The static apparatus and the experimental procedure for the VLE measurements have been improved and adopted to the high-pressure and high-dilution conditions.

The experimental *P–x* data at 323 K for water + 1-butanol, 2-butanol, 2-methyl-1-propanol, and 2-methyl-2-propanol systems have been measured. Our VLE and azeotropic results are in good agreement with the literature data. The evaluation of the activity coefficients at infinite dilution requires very high precision *P–x* values, especially at the high-dilution region. Our improved apparatus gives the required high-quality data. The values of the activity coefficients at infinite dilution obtained for the different butanols in water are higher than the values published by other researchers. With the apparatus described we can go to very high dilution, and it

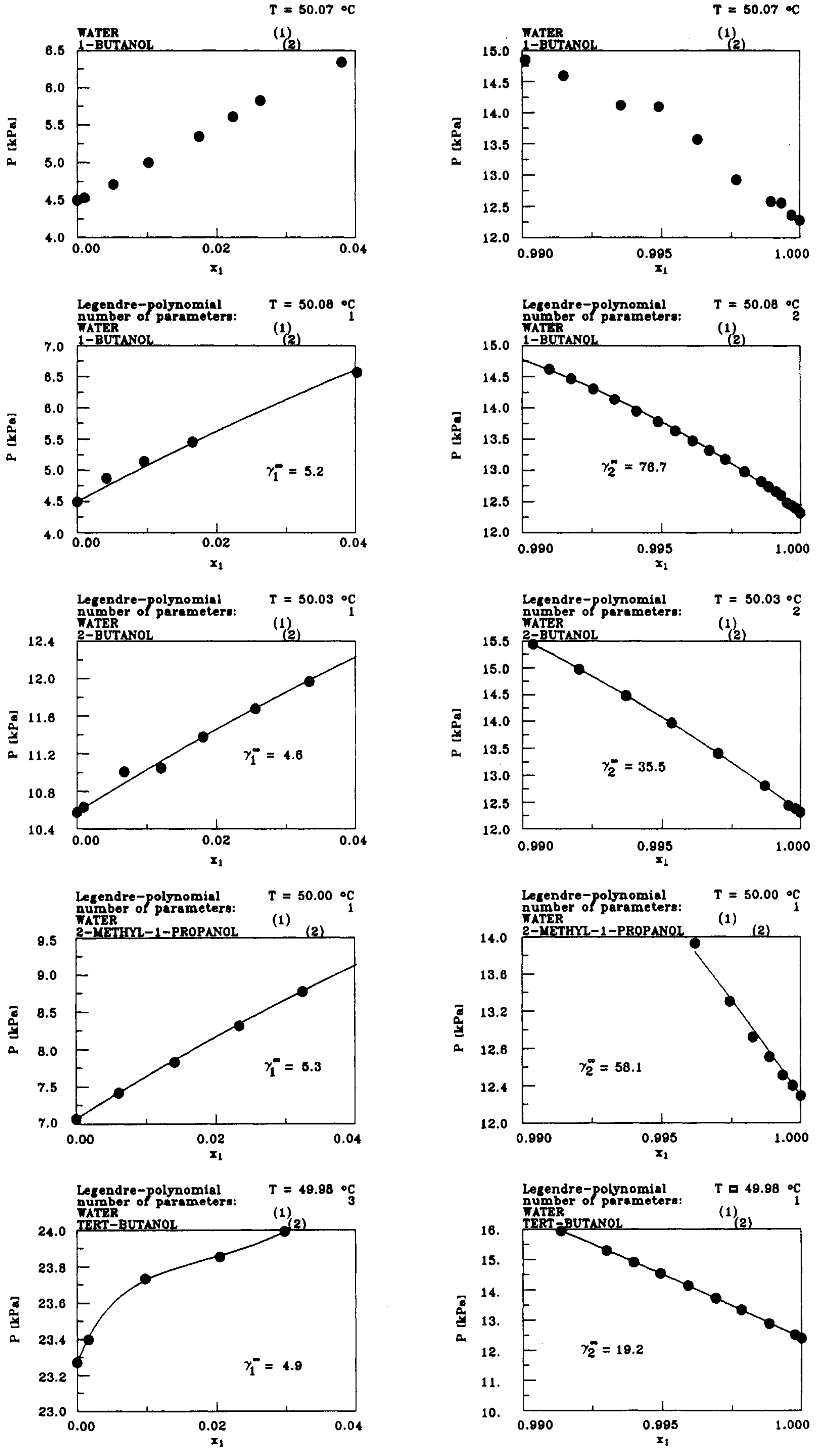

Figure 4. Experimental and calculated *P*–*x* data at high dilution using the Legendre polynomial.

has been well known that raising the dilution for water + alcohol mixtures leads to increasing values of the activity coefficients. Therefore we believe that the γ^∞ values given in this paper are more reliable. The data for the ethanol + water system have also been measured. The evaluated activity coefficients at infinite dilution show the same effect. The results for the ethanol + water mixture will be published soon (*13*).

Acknowledgment

The technical assistance of B. Meents is gratefully acknowledged.

Symbols

A, B, C	parameters for the Antoine equation
A_{ij}	parameter for G^E models (cal/mol)
F	objective function
G	molar Gibbs energy
P	pressure (kPa)
q	relative van der Waals surface area
r	relative van der Waals volume
T	temperature (K, °C)
x_i	mole fraction of component i in the liquid phase
y_i	mole fraction of component i in the vapor phase

Greek Symbols

α_{ij}	nonrandomness parameter
γ_i	activity coefficient of component i
Δ	difference (exptl − calcd)
ρ	density

Superscripts

E	excess property
s	saturation property
∞	at infinite dilution

Literature Cited

(1) Gmehling, J.; Onken, U.; Arlt, W.; Grenzheuser P.; et al. *Vapor-Liquid Equilibrium Data Collection*; DECHEMA Chemistry Data Series; DECHEMA: Frankfurt, first volume 1977; Vol. I, 18 parts.
(2) Van Ness, H. C.; Abbott, M. M. *Ind. Eng. Chem. Fundam.* **1978,** *17*, 66.
(3) Kolbe, B.; Gmehling, J. *Fluid Phase Equilib.* **1986,** *25*, 1.
(4) Nelder, J. A.; Mead, R. *Comput. J.* **1965,** *7*, 308.
(5) Kharin, S. E.; Perelygin, V. M.; Remizov, G. P. *Izv. Vyssh. Ucheb. Zaved., Khim. Khim. Tekhnol.* 1969, *12*, 424.
(6) Kentaemaa, J.; Tommila, E.; Martti, M. *Ann. Acad. Sci. Fenn.* **1953,** *AII*, 93.
(7) Lobien, G. M.; Prausnitz, J. M. *Ind. Eng. Chem. Fund.* **1982,** *21*, 109.
(8) Hofstee, M. T.; Kwantes, A.; Rijnders, C. W. A. Symposium Distillation Brighton, 1960; p 109.
(9) Mash, C. J.; Pemberton, R. C. NPL Report Chem. 111, July 1980.
(10) Ahlhorn, K. Praktikumsarbeit Dortmund. Unpublished data, 1986.
(11) Toome, M.; Kudryavtseva, L. S. *Zh. Fiz. Khim.* **1976,** *50*, 863.
(12) Altsybeeva, A. I.; Belousov, V. P.; Owtrakht, N. V.; et al. *Zh. Fiz. Khim.* **1964,** *38*, 1242.
(13) Fischer, K.; Gmehling, J. J. *Chem.Eng.Data*, in preparation.

Received for review July 9, 1993. Accepted November 1, 1993.[•] The authors thank "Fonds der Chemischen Industrie" for financial support of this work.

[•] Abstract published in *Advance ACS Abstracts,* January 1, 1994.